The Influence of Laser Nitriding on Creep Behavior of Ti-4Al-4V Alloy with Widmanstätten Microstructure

Luciana Aparecida Narciso da Silva Briguente [1,*], **Javier Oñoro** [2] , **Flávio Perpétuo Briguente** [3], **Fabrícia Assis Resende** [1], **Joares Lidovino dos Reis** [1,4], **Danieli Aparecida Pereira Reis** [1,5] and **Aline Capella de Oliveira** [1,*]

[1] Instituto de Ciência e Tecnologia, Universidade Federal de São Paulo (Unifesp)-Rua Talim, 330, São José dos Campos, SP 12231-280, Brazil; fabricia.aresende@gmail.com (F.A.R.); joares.lidovino@fatec.sp.gov.br (J.L.d.R.); danielireis@gmail.com (D.A.P.R.)

[2] ETSI Industriales, Universidad Politécnica de Madrid, C/José Gutiérrez Abascal, 2, 28006 Madrid, Spain; javier.onoro@upm.es

[3] International Society of Automation–Seção Vale do Paraíba-R. Argemiro dos Santos Filho, 152-Chácaras Selles, Guaratinguetá-SP, 12505-473, Brazil; fpbrigu@gmail.com

[4] Faculdade de Tecnologia Professor Jessen Vidal-Av. Cesare Mansueto Giulio Lattes, 1350, São José dos Campos, SP 12247-014, Brazil

[5] Department of Materials and Processes, Instituto Tecnológico de Aeronáutica—ITA/DCTA, São José dos Campos 12228-900, Brazil

* Correspondence: lunarsi@yahoo.com.br (L.A.N.d.S.B.); alinecapella@gmail.com (A.C.d.O.); Tel.: +1-251-472-5409 (L.A.N.d.S.B.); +55-12-3924-9500 (A.C.d.O.)

Abstract: Ti-6Al-4V alloy has been considered in applications of aeronautical and aerospace industries, due to its properties such as high specific resistance, good creep resistance and metallurgical stability. However, its use in applications for high temperatures is restricted due to its great affinity with the oxygen, which results in the formation of oxide layers and limits its mechanical resistance at these conditions. Thus, specific treatments have been employed in the material to work as surface barriers to avoid the oxygen diffusion in the alloy under high temperature conditions. One surface treatment that can be used is laser nitriding. In the present work, the surface of Ti-6Al-4V alloy with Widmanstätten microstructure was nitrided by applying Nd:YAG laser focal with 0.6 mm diameter, at laser power of 700, 750 and 800 W, process speed of 100 mm/s and 20 L/min of N_2 flow. Creep tests were performed at constant load at 600 °C and 125 MPa, to verify the influence of treatment on the Ti-6Al-4V alloy. Results have indicated a lower stationary creep rate for the titanium alloy with Widmanstätten laser-nitrided structure when compared to the non-nitriding material. Besides that, the surface hardness increased from 368 HV of base material to 1000 HV after laser nitriding.

Keywords: laser nitriding; Nd:YAG laser; creep; Ti-6Al-4V alloy

1. Introduction

Titanium and its alloys can be used in the aeronautics, aerospace, chemical biomedical among other industries, due to the combination of their mechanical resistance, high specific strength, corrosion resistance, low density, and biocompatibilities [1,2].

In particular, Ti-6Al-4V, with α + β phases, is one of the most important of titanium alloys, and has been widely used in the aeronautical and aerospace industries, particularly in applications that require resistance at high temperatures such as disks and blades for aircraft turbines and structural forgings. So, it is important to understand its properties and behavior in deformation under high temperatures [3,4].

However, the affinity of titanium alloys for oxygen when exposed to elevated temperatures during long-term use is one of the major factors for limiting the lifetime of the titanium alloy and for reducing their mechanical resistance [5,6]. In general, when titanium alloys are heated to temperatures above 800 °C, oxygen, hydrogen, and nitrogen can diffuse into the material, increasing its hardness and brittleness and reducing its tenacity [7]. Therefore, to employ these alloys under these conditions, the diffusion of oxygen must be reduced or controlled [5].

The titanium alloys interaction with oxygen causes loss of weight due to oxide formation and the embrittlement of the alloy by the dissolution of oxygen in the grain boundaries. This can reduce the material service lifetime when exposed to a combustion atmosphere composed of hot gases or corrosive media [6,8].

An alternative to increase Ti-6Al-4V lifetime and its working temperature is to apply coatings or use surface treatment on the material [9]. Some techniques that can be used for Ti-6Al-4V surface modification are physical vapor deposition (PVD), chemical vapor deposition (CVD), plasma spray coating (Thermal Barrier Coating), and plasma or laser surface treatments, including laser nitriding.

Laser nitriding works by melting the material surface. It uses a focused laser beam in a nitrogen atmosphere in order to form a hard titanium nitride layer on Ti-6Al-4V alloy. From the beam laser energy absorption, the substrate is heated, and the surface of the material is melted. Due to high temperature, results from laser-plasma-material interaction, the process of nitrogen ionization and dissociation can be done in the material. Dissolution of the nitrogen in the melted region allows the formation of titanium nitride dendrites [10]. It is an attractive technique that provides an excellent metallurgical bond between the nitride layer and the substrate [11]. Besides that, it can improve its mechanical and tribological properties, and create a barrier avoiding inward oxygen diffusion and increase the oxidation resistance of titanium alloys [12].

Ti-6Al-4V alloy exhibits two important types of microstructure. The first one is an equiaxial alpha structure with β-phase in the grain boundaries, obtained after annealing treatment. The other one is referred to as Widmanstätten, and it is a coarser α-phase lamellar structure formed from the β-grain boundaries. This microstructure is obtained after slow cooling into the two-phase region (1050 °C), leads to nucleation and growth of the alpha-phase in plate form starting from beta-grain contours [13]. Among these microstructures, Widmanstätten presents the greatest creep resistance [14]. This higher creep resistance of the Ti-6Al-4V alloy with Widmanstätten microstructure can be attributed to the α/β interfaces acting as obstacles to the dislocation motion and due to the larger initial average grain size, which reduces the grain boundary sliding, dislocation sources and the rate of oxygen along the grain boundaries [13].

An important parameter for materials used as structural components is the creep resistance. This is a limiting parameter in design under different temperature-stress domains [15]. Ti-6Al-4V creep researches have been well documented due to its technological importance [8,14,16–18].

Creep behavior of Ti-6Al-4V with equiaxed structure nitriding by pulsed Nd:YAG laser was studied by Reis, A.G., 1012 [17]. Briguente, L. A. N. S. 2011 [14] analyzed creep behavior of Ti-6Al-4V with Widmanstätten structure and it was found out that this microstructure has higher creep resistance when compared to equiaxial microstructure, resulting in a steady-state creep rate decrease from 0.0410 to 0.0014 (1/h) at stress of 125 MPa and temperature of 600 °C [14]. However, there is no study related to the creep behavior of Ti-6Al-4V with Widmanstätten nitrided-surface structure by Nd:YAG laser reported in the literature.

The present work aims to study creep behavior of Ti-6Al-4V with Widmanstätten nitrided-surface structure by continuous Nd:YAG laser. Mechanical tests were performed at 600 °C and 125 MPa, considering different laser power conditions. Microstructural changes caused by laser nitriding are evaluated by scanning electron microscopy and energy dispersive X-ray spectroscopy. Titanium nitride formation was confirmed by X-Ray diffraction and laser effects on surface hardness are still under investigation.

2. Experimental Procedures

The material used in this work was a hot-forged 12.7 mm diameter rod of commercial Ti-6Al-4V alloy. The microstructure of the received material was Widmanstätten microstructure, obtained by heating the material above β transformation temperature and holding at 1050 °C for 30 min, followed by furnace cooling to 700 °C for 1 h and air cooled to room temperature. This heat treatment was conducted in argon atmosphere.

The specimens for creep tests were prepared with a gauge length of 18.5 mm and a diameter of 3.0 mm, according to ASTM E139-06 [19]. To obtain creep elongation measures, it was used a transducer, type LVDT Schlumberger D 6.50 (Daytronic, Miamisburg, OH, USA). The LVDT output signal was sent to a processing unit, which converts the signals into deformation and these measures were sent to a software.

Laser nitriding was carried out using a diode pumped Nd:YAG continuous laser, Rofin DY033 (Plymouth, MI, USA), with 1 μm wavelength. The laser nitriding was performed with the laser spot size, with a diameter of 0.6 mm, focused on surface material, considering laser power of 700, 750 and 800 W, process speed of 100 mm/s and nitrogen at a flow rate of 20 L/min. The laser intensities varied between 2475.7 and 2828.4 W/mm^2. Nitriding was performed without overlapping of the laser beam on the material surface.

Creep behavior of the laser-nitrided Ti-6Al-4V alloy with Widmanstätten structure was compared to untreated material by tests conducted in a standard Mayes creep machine, according to ASTM E139-06 [19]. Constant load creep tests were conducted in air atmosphere at stress level of 125 MPa and a temperature of 600 °C. Constant creep parameters were considered in this study to evaluate the influence of laser parameters on the behavior material submitted to creep conditions. The creep parameters applied in the present study were based on previous works of the authors, such as: [8,13,14,17,18].

After tests, fractographic analysis was performed in a scanning electron microscopy (SEM) (FEI, Hillsboro, OR, USA) to identify creep fracture mechanism.

Metallographic analysis was done on samples at longitudinal section and cross-sectional by scanning electron microscopy (SEM) combined to energy dispersive spectroscopy (EDS) using a TESCAN FEG microscope MIRA 3 model (Tescan, Brno, Czech Republic). Material surface microhardness (top surface, thermally affected zone and base material) of cross-sectional plane was measured by a Vickers hardness tester using loads of 50 gf up to 100 gf. Vickers microhardness tests were conducted in the cross section of creep test sample in regions which cover the melted region, heat affected zone, grain growth region and base material.

3. Results and Discussion

3.1. Microstructure Evaluation

Ti-6Al-4V Widmanstätten microstucture is a coarser α-phase lamellar structure formed from the β-grain boundaries. Figure 1 shows an optical micrograph of this structure.
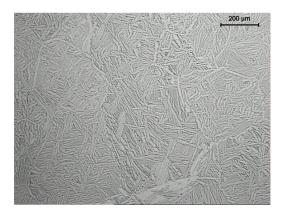

Figure 1. Optical micrograph of Widmanstätten microstructure.

The microstructure of Ti-6Al-4V with Widmanstätten microstructure after laser nitriding is shown in Figures 2–4 and it is possible to identify a modification of its morphology. The microstructure of the nitreted surface consists of a laser melted region, a heat affected zone (HAZ), and a region with an increase of the grain size and the substrate. The microstructure of the laser melted region consists of a thin layer followed by a growth of TIN dendrites [20]. The Heat affected zone (HAZ) is found after the melted zone and it is formed by needle-shaped structures called titanium martensite (Ti-α'). This occurs due to the laser-material interaction that increases the temperature up to β-phase field. After its quick cooling, the martensitic transformation in this region is observed [9]. An increase of average grain size in the Heated Affected Zone is also observed, after laser nitriding of the Ti6Al4V with Widmanstatten microstructure. This can be related to higher temperatures in the material, that can cause diffusion along the grain boundaries and increase their size. This behavior is beneficial in the material creep resistance. A smaller grain boundary area, is related to a lower oxygen diffusion along the grain boundaries [13,14,21].
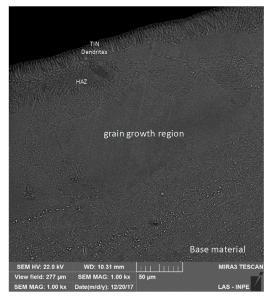

Figure 2. Longitudinal SEM of Widmanstätten microstructure after laser nitriding. Laser Power: 700 W.
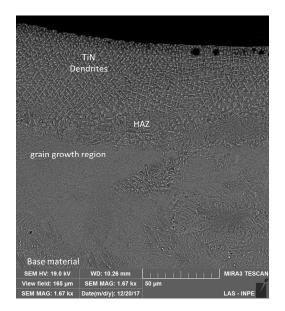

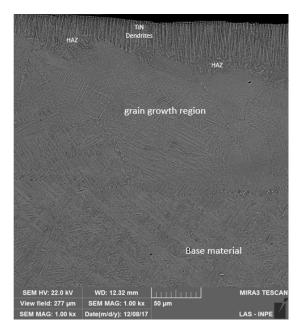**Figure 3.** Longitudinal SEM of Widmanstätten microstructure after laser nitriding. Laser Power: 750 W.

Figure 4. Longitudinal SEM of Widmanstätten microstructure after laser nitriding. Laser Power: 800 W.

3.2. Hardness of Nitrided Material

The hardness at regions of the nitrided material was measured. Figure 5 shows the results obtained to different process conditions. Increased hardness in the laser melted region could be observed, where the values found are between 900 and 1000 HV. This behavior can be attributed to TIN layers formed during the nitriding process, where the higher hardness near the surface is attributed to the higher nitrogen concentration on the region. In the thermal affected zone, the hardness is reduced to order 675 HV, which can be attributed to the presence of martensitic Ti-α' phase. The grain growth region has higher hardness (470 HV on average) when compared to the base material (368 HV on average). This can be attributed to nitrogen diffusion in small volumetric fraction. However, the nitrogen diffusion in this region could not be observed by the applied characterization techniques.

ABBOUD, J. H., et al., 2008 [22] investigated the surface nitriding of a Ti-6Al-4V alloy by the use of a high-power CO_2 laser in a flow of nitrogen, and the hardness was about 1350 HV to a shallow depth 50–80 μm below the surface, and the microhardness decreased to 800 HV for a depth 0.4 mm below the surface. REIS, 2013, [20] observed higher hardness value in the nitrided Ti-6Al-4V with equiaxial microstructure with values of 1100 VHN. CHAN, C. W., et al., 2017 [23] performed a nitriding using a continuous wave fibre laser in Ti-6Al-4V (TIG5) alloy. The result found was 977 ± 108 HV for the nitrided area and 652 ± 269 HV. So, the results found in the present work are according to the literature.
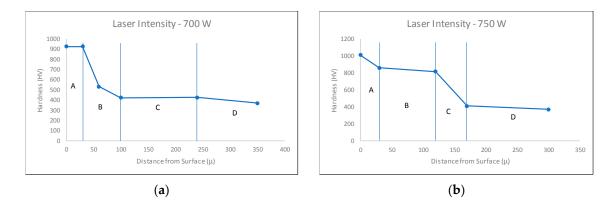

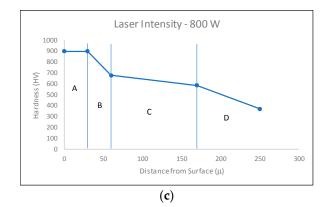
(**a**)

(**b**)

Figure 5. *Cont.*

(**c**)

Figure 5. Hardness profile of Ti-6Al-4V alloy after nitriding process: (A) Melted region; (B) Heat affected zone; (C) Grain growth region; (D) Base material. (**a**) Laser Intensity—700 W; (**b**) Laser Intensity—750 W; (**c**) Laser Intensity—800 W.

3.3. Creep Tests

The creep tests were conducted on Ti-6Al-4V alloy for the received Widmanstätten microstructure specimens and on the laser nitrided specimens, considering the load (125 MPa) and temperature (600 °C). The creep curves (Figure 6) exhibit normal behavior which consists of well-defined primary, secondary and tertiary stages. A short initial period with a decrease at the primary creep rate could be observed, that is associated with the hardening process due to the accumulation of dislocations. However, a constant creep rate is observed at a larger period of creep life. This can be associated with a balance between the recovery and hardening process [13].

The results from creep tests are summarized in Table 1, which show the values of the primary creep time t_p, secondary creep rate $\dot{\varepsilon}_s$, and the time to rupture (t_r). Comparing the results between base material and nitrided material specimens, a reduction of secondary creep rate for all laser nitriding conditions is observed. TIN layer act as barrier against oxygen diffusion into the alloy, improving its creep resistance [12]. Secondary creep rate decreased from 0.0014 to 0.000522 1/h and 0.000465 1/h at 700 W and 800 W laser power respectively.

The final fracture time is higher for the nitrided specimens with 700 W and 750 W when compared to the fracture time of the base material specimens, which indicates improvement in the material mechanical behavior. In this case, the final fracture time of the nitrided alloy with power of 750 W was about two times higher than the fracture time for the untreated alloy. At 800 W the time to fracture is 98.7 h, lower than the other conditions. This can be associated with the thicker nitrided layer, that is beneficial as a thermal barrier and, therefore, directly influences the secondary creep rate but adversely increases material hardness in this region and reduces the creep time to fracture.
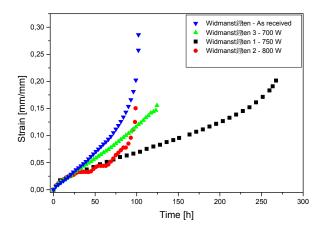

Figure 6. Creep Curves at 600 °C and 125 MPa of Ti-6Al-4V before and after laser nitriding.

ε_f (mm/mm) represents the specimen's deformation after creep tests. This value is related with the type of fracture in creep tests. A higher value is observed in ductile fracture, as shorter value is observed at fragile fracture. As can be observed in Table 1, a higher value can be observed in material as received (no laser treatment). Laser nitriding can be a thermal barrier and decrease oxygen diffusion but can interfere on material ductility and decrease its deformation after creep tests.

Table 1. Creep data at 600 °C and 125 MPa of Ti-6Al-4V before and after laser nitriding.

Laser Power W	t_p (h)	$\dot{\varepsilon}_s$ (1/h)	t_f (h)	ε_f (mm/mm)
As received	9.00	0.00140	102.12	0.2861
700	2.48	0.00110	124.38	0.1555
750	2.65	0.000522	272.40	0.2348
800	2.83	0.000465	98.70	0.1504

Creep tests conducted in this study are short term creep tests, that evaluate creep behavior in conditions of high temperatures or stress levels. In these conditions creep behavior of applications that can occasionally demand short-time exposures is evaluated. Because of this, it is important to have data on the material creep behavior during these service conditions. All the specimens were tested until fracture.

An EDS analysis was carried out after creep trials in the fractured specimens and the results are shown in Tables 2–4. A nitrogen concentration at depth from 8 to 38 μm can be observed, and oxygen can be detected because the analysis was conducted after creep tests, which takes place in an oxidant environment. The nitrogen presence after creep trials confirm that nitriding process was efficient.

Table 2. EDS data after creep test of Ti6Al4V nitrided with 750 W of laser power.

Depth	% of elements (wt.)				
	Ti	Al	V	O	N
18 μm	85.2	1.9	2.0	5.5	5.4
24 μm	86.9	4.1	2.1	4.8	2.1
30 μm	85.1	3.6	3.1	5.3	2.9

Table 3. EDS data after creep test of Ti6Al4V nitrided with 800 W of laser power.

Depth	% of elements (wt.)				
	Ti	Al	V	O	N
9 μm	81.0	1.8	2.2	8.7	6.3
13 μm	84.8	3.9	3.5	5.8	2.0
17 μm	85.4	4.0	2.7	6.1	1.8
33 μm	86.3	3.9	3.1	4.9	1.8

Table 4. EDS data after creep test of Ti6Al4V nitrided with 700W of laser power.

Depth	% of elements (wt.)				
	Ti	Al	V	O	N
8 μm	84.2	2.2	2.3	6.3	5.0
18 μm	84.2	3.9	4.4	5.5	2.0
38 μm	86.3	3.0	2.5	5.7	2.5

3.4. Fracture Surfaces

Post creep test fracture surfaces of Ti-6Al-4V specimens are shown in Figure 7. The fracture mode has exhibited ductile fracture mechanism with the narrowing phenomenon and development of

microcavities in the central region of the fractured specimens. The test conditions were characterized by the formation and coalescence of microcavities with different sizes and shapes, with the deepest present in the central region of the sample. Specially, in the condition of higher laser power (800 W), smooth marks of deformation are observed in the edges of the specimen, with fragile characteristics. This is in accordance with shorter fracture time observed for the highest power condition used for the laser nitriding process, which reduces the material ductility in this region.
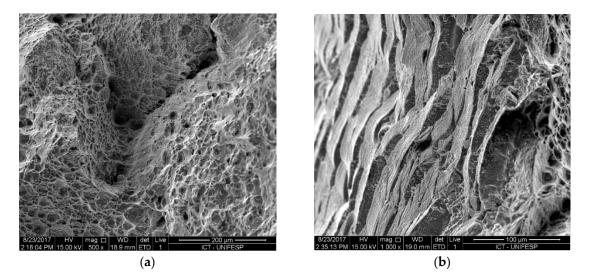

Figure 7. SEM micrographs showing surfaces after creep tests at 600 °C, 125 MPa and laser intensity of 2829 W/mm^2. (**a**) central region of creep test; (**b**) creep test border.

4. Conclusions

The surface nitriding of a Ti-6Al-4V with Widmanstätten structure was conducted with a continuous Nd:YAG laser. It can be concluded that surface laser-nitriding techniques can improve the creep resistance of the Ti-6Al-4V alloy with Widmanstätten structure.

- The microstructure of the nitrided surface consisted of a laser melted region, a heat affected zone (HAZ) formed by needle-shaped structures called titanium martensite (Ti-α'), and a region with an increase of the grain size and the substrate. An improvement in hardness (900–1000 HV) in comparison to the base material (368 HV) was observed.
- A reduction of secondary creep rate for all laser nitriding conditions was observed. TIN layer acts as a barrier against oxygen diffusion into the alloy, improving its creep resistance. The final fracture time is higher for 700 and 750 W laser nitrided specimens when compared to the fracture time of the base material, which indicates improvement of the material mechanical behavior. At 800 W, the time to fracture is lower than the other conditions, and this can be associated with the thicker nitrided layer, that increases material hardness in this region and reduces the creep time to fracture.
- EDS analysis conducted after creep trials in the fractured specimens showed a nitrogen concentration at a depth from 8 to 38 μm, that can confirm an efficient nitriding process.
- Post creep tests fracture surfaces exhibited ductile fracture mechanism with the narrowing phenomenon and development of microcavities in the central region of the fractured specimens.

Conflicts of Interest: The authors declare no conflict of interest.

References

1. Leyens, C.; Peters, M. *Titanium and Titanium Alloys: Fundamentals and Applications*; Wiley-VCH Verlag GmbH & Co. KGaA: Weinheim, Germany, 2003; 449p, ISBN 9783527305346.

2. International Titanium Association. *Titanium Facts*; International Titanium Association: USA, 2007; Available online: www.titanium.org (accessed on 10 February 2019).

3. Sakai, T.; Ohashi, M.; Chiba, K.; Jonas, J.J. Recovery and recrystallization of Polycrystalline nickel after hot working. *Acta Metall.* **1988**, *36*, 1781–1790. [CrossRef]

4. Lee, W.S.; Lin, C.F. High temperature deformation behavior of Ti-6Al-4V alloy evaluated by strain-rate compression tests. *J. Mater. Process. Technol.* **1998**, *75*, 127–136. [CrossRef]

5. Gurrappa, I.; Gogia, A.K. High performance coatings for titanium alloys to protect against oxidation. *Surf. Coat. Technol.* **2001**, *139*, 216–221. [CrossRef]

6. Sai Srinadh, K.V.; Singh, V. Oxidation behaviour of the near α-titanium alloy IMI 834. *Bull. Mater. Sci.* **2004**, *27*, 347–354. [CrossRef]

7. Rosenand, A.R. The effect of high temperature exposure on the creep resistance of Ti-6Al-4V alloy. *Mater. Sci. Eng.* **1976**, *22*, 23–29.

8. Reis, D. Estudo de recobrimento cerâmico e da atmosfera de ensaio na fluência de liga metálica refratária de titânio. Ph.D. Thesis, Instituto Nacional de Pesquisas Espaciais, São José dos Campos, Brazil, 30 September 2005.

9. Akgnun, O.V.; Inal, O.T. Laser surface melting of Ti-6Al-4V alloy. *J. Mater. Sci.* **1992**, *27*, 1404–1408. [CrossRef]

10. Zielinski, A.; Jazdzewska, M.; Narozniaki-Luksza, A.; Serbinski, W. Surface structure and properties of Ti-6Al-4V alloy laser melted at cryogenic conditions. *J. Achiev. Mater. Manuf. Eng.* **2006**, *18*, 423–426.

11. Zecheva, A.; Sha, W.; Malinov, S.; Long, A. Enhancing the microstructure and properties of titanium alloys through nitriding and other surface engineering methods. *Surf. Coat. Technol.* **2005**, *200*, 2192–2207. [CrossRef]

12. Perez, P. Influence of nitriding on the oxidation behavior of titanium alloys at 700 °C. *Surf. Coat. Technol.* **2005**, *191*, 293–302. [CrossRef]

13. Barboza, M.J.R.; Perez, E.A.C.; Medeiros, M.M.; Reis, D.A.P.; Nono, M.C.A.; Piorino Neto, F.; Silva, C.R.M. Creep behavior of Ti-6Al-4V and a comparison with titanium matrix composites. *Mater. Sci. Eng. A* **2006**, *428*, 319–326. [CrossRef]

14. Briguente, L.A.N.d.S. Estudo de tratamento térmico e recobrimento como forma de barreira térmica sobre o comportamento em fluência da liga Ti-6Al-4V. Master's Thesis, Instituto Tecnológico de Aeronáutica, São José dos Campos, Brazil, 25 May 2011.

15. Evans, R.W.; Wilshire, B. *Introduction to Creep*; The Institute of Materials: London, UK, 1993; 115p.

16. Barboza, M.J.R.; Moura Neto, C.; Silva, C.R.M. Creep mechanisms and physical modeling for Ti-6Al-4V. *Mater. Sci. Eng. A* **2004**, *369*, 201–209. [CrossRef]

17. Reis, G. Avaliação do comportamento em fluência da liga Ti-6Al-4V submetida ao tratamento superficial de nitretação por laser. Master's Thesis, Instituto Tecnológico de Aeronáutica, São José dos Campos, Brazil, 2 March 2012.

18. Briguente, F.P. Estudo dos Recobrimentos Metálico e Cerâmico no comportamento em fluência da liga Ti-6Al-4V. Ph.D. Thesis, Instituto Tecnológico de Aeronáutica, São José dos Campos, Brazil, 15 April 2015.

19. American Society for Testing and Materials (ASTM) E139-06. *Standard Practice for Conducting Creep, Creep-Rupture and Stress-Rupture Tests of Metallic Materials*; American Society for Testing and Materials: West Conshohocken, PA, USA, 2006.

20. Reis, A.G.; Reis, D.A.P.; de Moura Neto, C.; Barboza, M.J.R.; Oñoro, J. Creep behavior and surface characterization of a laser surface nitrided Ti-6Al-4V alloy. *Mater. Sci. Eng. A* **2013**, *577*, 48–53. [CrossRef]

21. Venkatesh, T.A.; Conner, B.P.; Suresh, S.; Giannakopoulos, A.E.; Lindley, T.C.; Lee, C.S. An Experimental Investigation of Fretting Fatigue in Ti-6Al-4V: The Role of Contact Conditions and Microstructure. *Metall. Mater. Trans. A* **2001**, *32A*, 1131–1146. [CrossRef]

22. Abboud, J.H.; Fidelg, A.F.; Benyounisc, K.Y. Surface nitriding of Ti-6Al-4V alloy with a high power CO_2 laser. *Opt. Laser Technol.* **2008**, *40*, 405–414. [CrossRef]

23. Chan, C.-W.; Lee, S.; Smith, G.C.; Donaghy, C. Fibre laser nitriding of titanium and its alloy in open atmosphere for orthopaedic implant applications: Investigations on surface quality, microstructure and tribological properties. *Surf. Coat. Technol.* **2017**, *309*, 628–640. [CrossRef]